Journal of Enzyme Inhibition and Medicinal Chemistry, 2010; 25(1): 87–96

informa
healthcare

RESEARCH ARTICLE

DNA cleavage and in vitro antimicrobial studies of Co(II), Ni(II), and Cu(II) complexes with ONNO donor Schiff bases: Synthesis, spectral characterization, and electrochemical studies

Ajaykumar Kulkarni[1], Sangamesh A. Patil[1], and Prema S. Badami[2]

[1]*P.G. Department of Chemistry, Karnatak University, Dharwad, Karnataka, India, and* [2]*Department of Chemistry, Shri Sharanabasaveswar College of Science, Gulbarga, Karnataka, India*

Abstract

A series of Co(II), Ni(II), and Cu(II) complexes of the type $ML.2H_2O$ have been synthesized with Schiff bases derived from 8-formyl-7-hydroxy-4-methylcoumarin and *o*-phenylenediamine/ethylenediamine. The structure of the complexes has been proposed in the light of analytical, spectral (IR, UV-Vis, ESR, and FAB-mass), magnetic, thermal, and fluorescence studies. The complexes are soluble in DMF and DMSO. The measured molar conductance values indicate that the complexes are non-electrolytes in nature. In view of IR, UV-Vis, and magnetic studies, it has been concluded that all the complexes possess octahedral geometry, in which ligand is coordinated to metal ion through the azomethine nitrogen and phenolic oxygen via deprotonation. Thermal studies provide useful information about the coordination of water molecules to the metal ion and the stability of the complexes. The redox behavior of the complexes has been investigated by an electrochemical method using cyclic voltammetry. The Schiff bases and their metal complexes have been screened for their antibacterial (*Escherichia coli*, *Staphylococcus aureus*, *Pseudomonas aeruginosa*, and *Salmonella typhi*) and antifungal activities (*Aspergillus niger*, *Aspergillus flavus*, and *Cladosporium*) by the minimum inhibitory concentration method. DNA binding with Co(II) and Cu(II) complexes has been studied by the agarose gel electrophoresis method.

Keywords: *Coumarin; cyclic voltammetry; DNA; microbial; spectral; synthesis; metal complexes*

Introduction

Coumarin is structurally the least complex member of a large class of compounds known as benzopyrones[1]. Coumarin derivatives possess a wide range of biological activities, viz. antithrombotic[2], antimicrobial[3], antiallergic[4], antiinflammatory[5], antitumor[6], and anticoagulant[7], etc. Recently, coumarin derivatives have been evaluated in the treatment of human immunodeficiency virus (HIV), due to their ability to inhibit HIV integrase[8,9]. *In vitro* and *in vivo* studies have suggested the possible use of coumarins in the treatment of cancer[10]. The coumarin nucleus is also present in the novobiocin, clorobiocin, and coumermycin A_1 antibiotics. These antibiotics are active against methicillin-resistant *Staphylococcus aureus*[3] and are potent catalytic inhibitors of DNA gyrase. The interaction of transition metal complexes with DNA has been extensively studied for their usage as probes for DNA structure and their potential application in chemotherapy[11–13]. One of the important DNA-related activities of transition metal complexes is that some of the complexes show the ability to cleave DNA. Very recently, Cu(II) complexes have been reported to be active in DNA strand scission[14–16].

Such a wide spectrum of biological application of coumarins prompted us to synthesize some of the transition metal complexes with coumarin Schiff bases. Very recently, metal complexes with coumarin Schiff bases possessing good antimicrobial activity have been reported from our laboratory[17,18].

Address for Correspondence: Sangamesh A. Patil, P.G. Department of Chemistry, Karnatak University, Dharwad-580003, Karnataka, India. Fax: 91 (0836) 2771275. E-mail: patil1956@rediffmail.com

(Received 04 December 2008; revised 08 March 2009; accepted 01 April 2009)

ISSN 1475-6366 print/ISSN 1475-6374 online © 2010 Informa UK Ltd
DOI: 10.3109/14756360903017791

Thus, in continuation with our earlier work, we report here the antimicrobial activity and DNA cleavage property of Co(II), Ni(II), and Cu(II) metal complexes with newly synthesized Schiff bases derived from 8-formyl-7-hydroxy-4-methylcoumarin and *o*-phenylenediamine/ethylenediamine (Scheme 1). The Schiff bases and their metal complexes have been characterized by various spectral and analytical techniques.

Experimental

Physical measurements

Carbon, hydrogen, and nitrogen were estimated using a Carlo Erba EA1108 elemental analyzer. The infrared (IR) spectra of the Schiff bases and their Co(II), Ni(II), and Cu(II) complexes were recorded on a Hitachi 270 IR spectrophotometer in the 4000–250 cm^{-1} region using a KBr disk. The electronic spectra of the complexes were recorded in high performance liquid chromatography (HPLC) grade dimethylformamide (DMF) and dimethylsulfoxide (DMSO) solvents on a Varian Cary 50-Bio ultraviolet (UV) spectrophotometer in the region of 200–1100 nm. The ^{1}H nuclear magnetic resonance (NMR) and ^{13}C NMR spectra of the Schiff bases were recorded in $CDCl_3$ on a Bruker 300 MHz spectrometer at room temperature, using tetramethylsilane (TMS) as an internal reference. The electron spin resonance (ESR) spectrum was recorded on a Varian E-4X band spectrometer, and the field was set at 3000 G at a modulation frequency of 100 kHz under liquid nitrogen temperature using tetracyanoethylene (TCNE) as g-marker. Fast atom bombardment (FAB)-mass spectra were recorded on a Jeol SX 102/DA-6000 mass spectrometer/data system using argon/xenon (6 kV, 10 A) as the FAB gas. The accelerating voltage was 10 kV, and the spectra were recorded at room temperature and *m*-nitrobenzyl alcohol was used as the matrix. The mass spectrometer was operated in the positive ion mode. Fluorescence studies of Schiff bases and their metal complexes were recorded on a Hitachi F-7000 fluorescence spectrophotometer (Japan). Solutions (10^{-3} M concentration) were prepared in HPLC grade DMF and DMSO solvents and the experiment was carried out at room temperature. The electrochemistry of Cu(II) complexes was studied on a CH Instruments 1110A electrochemical analyzer (USA) in DMF containing 0.05 M *n*-Bu_4NClO_4 as the supporting electrolyte. The three-electrode system consisted of a glassy carbon electrode (3 mm diameter) as a working electrode, an Ag/AgCl (3 M KCl) reference electrode, and a platinum wire as auxiliary electrode. Thermogravimetric analysis data were measured from room temperature to 1000°C at a heating rate of 10°C/min. The data were obtained using a PerkinElmer Diamond TG/DTA instrument. Molar conductivity measurements were recorded on an Elico-CM-82 T conductivity bridge with a cell constant 0.51, and magnetic moment determination was carried out using a Faraday balance.

Synthesis

All the chemicals used were of reagent grade. 7-hydroxy-4-Methylcoumarin was synthesized according to the literature procedure[19].

Synthesis of 8-formyl-7-hydroxy-4-methylcoumarin

8-Formyl-7-hydroxy-4-methylcoumarin was prepared by the known method[17]. 7-Hydroxy-4-methylcoumarin (0.03 mol) and hexamine (0.07 mol) in glacial acetic acid (50 mL) were heated for 4–5 h, then 20% HCl (75 mL) was added and the mixture further heated for 20 min, then cooled and extracted with ether. The pale yellow-colored solid of 8-formyl-7-hydroxy-4-methylcoumarin that was

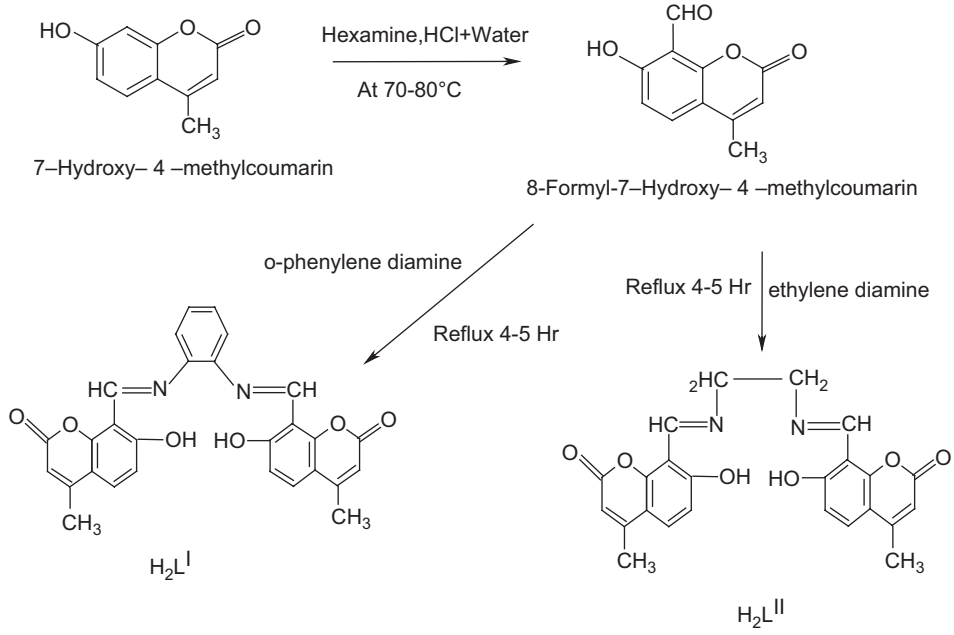

Scheme 1. Synthesis of Schiff bases $\mathbf{H_2L^I}$ and $\mathbf{H_2L^{II}}$.

obtained after extraction was recrystallized from hot ethanol: m.p. 176–177°C, yield 2.5 g.

Synthesis of Schiff bases H_2L^I and H_2L^{II}

The Schiff bases were synthesized by refluxing the reaction mixture of hot ethanol solution (30 mL) of *o*-phenylenediamine/ethylenediamine (0.01 mol) and hot ethanol solution (30 mL) of 8-formyl-7-hydroxy-4-methylcoumarin (0.02 mol) for 4–5 h with the addition of 2–3 drops of hydrochloric acid. The precipitate that formed during reflux was filtered, washed with cold EtOH, and recrystallized from EtOH.

Synthesis of Co(II), Ni(II), and Cu(II) complexes (1–6)

An alcoholic solution (45 mL) of Schiff base (1 mmol) was mixed with an alcoholic solution (10 mL) of 1 mmol of $CoCl_2.6H_2O$/$NiCl_2.6H_2O$/$CuCl_2.2H_2O$ and refluxed on a water bath for 2 h. Then, to the reaction mixture, 2 mmol of sodium acetate was added and reflux was continued for 3 h. The separated complex was filtered, washed thoroughly with water, ethanol, and ether, and finally dried under vacuum over fused $CaCl_2$.

Preparation of culture media

Nutrient broth (peptone, 10; yeast extract, 5; NaCl, 10; in g/L) was used for culturing of *Escherichia coli* and potato dextrose broth (potato, 250; dextrose, 20; in g/L) was used for the culture of *Aspergillus niger*. Media (50 mL) were prepared, and autoclaved for 15 min at 121°C under 15 lb pressure. The autoclaved media were inoculated with the seed culture. *E. coli* was incubated for 24 h and *A. niger* for 48 h at 37°C.

Isolation of DNA

The fresh bacterial culture (1.5 mL) was centrifuged to obtain a pellet which was then dissolved in 0.5 mL of lysis buffer (100 mM Tris, pH 8.0, 50 mM EDTA (ethylenediaminetetraacetic acid), 10% SDS (sodium dodecyl sulfate)). To this, 0.5 mL of saturated phenol was added and the mixture was incubated at 55°C for 10 min then centrifuged at 10,000 rpm for 10 min, and to the supernatant, an equal volume of chloroform–isoamyl alcohol (24:1) and one-twentieth volume of 3 M sodium acetate (pH 4.8) were added. The mixture was centrifuged at 10,000 rpm for 10 min, and to the supernatant, three volumes of chilled absolute alcohol were added. The precipitated DNA was separated by centrifugation, and the pellet was dried and dissolved in TAE buffer (10 mM Tris, pH 8.0, 1 mM EDTA) and stored in cold conditions.

DNA cleavage experiment

DNA cleavage experiments were done according to the literature procedure[20].

Agarose gel electrophoresis

Cleavage products were analyzed by the agarose gel electrophoresis method[20]. Test samples (1 mg/mL) were prepared in DMF. Samples (25 μg) were added to the isolated DNA of *E. coli* and *A. niger*. The samples were incubated for 2 h at 37°C, and then 20 μL of the DNA sample (mixed with bromophenol blue dye in a 1:1 ratio) was loaded carefully into the electrophoresis chamber wells along with standard DNA marker containing TAE buffer (4.84 g Tris base, pH 8.0, 0.5 M EDTA/L) and finally loaded on agarose gel, and a constant 50 V of electricity was passed for around 30 min. The gel was removed and stained with 10.0 μg/mL ethidium bromide for 10–15 min, and the bands observed under a Vilberlourmate gel documentation system and photographed to determine the extent of DNA cleavage. The results were then compared with standard DNA marker.

In vitro antibacterial and antifungal assay

The biological activities of synthesized Schiff bases and their Co(II), Ni(II), and Cu(II) complexes have been studied for their antibacterial and antifungal activities by agar and potato dextrose agar diffusion methods, respectively, in DMF solvent against *Escherichia coli*, *Staphyllococcus aureus*, *Psuedomonas aeruginosa*, and *Salmonella typhi* bacterial species and *Aspergillus niger*, *A. flavus*, and *Cladosporium* fungal species[21]. A stock solution (1 mg/mL) of test chemical was prepared by dissolving 10 mg of the test compound in 10 mL of DMF solvent. The stock solution was suitably diluted with sterilized distilled water to obtain concentrations of of 100, 50, and 25 μg/mL. A control for each dilution was prepared by diluting 10 mL of solvent instead of stock solution with sterilized distilled water.

The bacteria were subcultured in agar medium. Petri dishes were incubated for 24 h at 37°C. The standard antibacterial drug, gentamicin, was also screened under similar conditions for comparison. The fungi were subcultured in potato dextrose agar medium. The standard antifungal drug, fluconazole, was used for comparison. Petri dishes were incubated for 48 h at 37°C. Sterile disks were used in the agar media. Activity was determined by measuring the diameter of the zone showing complete inhibition (mm).

Compounds showing promising antibacterial/antifungal activity were selected for minimum inhibitory concentration (MIC) studies[21].

Results and discussion

The synthesis of Schiff bases is schematically presented in Scheme 1. The Schiff bases $\mathbf{H_2L^I}$ and $\mathbf{H_2L^{II}}$ with $CoCl_2.6H_2O$/$NiCl_2.6H_2O$/$CuCl_2.2H_2O$ in EtOH give octahedral complexes (**1–6**) where the coordination sphere of the central metal ion is occupied by two water molecules. All the Co(II), Ni(II), and Cu(II) complexes were colored, stable, and non-hygroscopic in nature. The complexes were insoluble in common organic solvents but soluble in DMF and DMSO. The elemental analyses showed that the Co(II), Ni(II), and Cu(II) complexes have 1:1 stoichiometry of the type $ML.2H_2O$, where L stands for a doubly deprotonated ligand. The molar conductance values are too low to account for any dissociation of the complexes in DMF, indicating the non-electrolytic nature of the complexes in DMF (Table 1).

Infrared spectra

The prominent infrared spectral data of Schiff bases and their Co(II), Ni(II), and Cu(II) complexes are presented in Table 2.

The IR spectra of the Schiff bases exhibited a characteristic high-intensity band at 1613–1632 cm^{-1}, which is attributed to the ν(C=N) vibration[22]. The broad band around 3072–3062 cm^{-1} and a strong band at 1306–1305 cm^{-1} in the spectra of the Schiff bases are assigned to H-bonded –OH stretching and phenolic ν(C-O) vibrations, respectively. Another strong band at 1735–1720 cm^{-1} is assigned to ν(C=O), the lactonyl carbon of the coumarin moiety[23].

In comparison with the spectra of the Schiff bases, all the complexes exhibited the band of ν(C=N) in the region 1598–1622 cm^{-1}; the shift of the band to lower wave numbers[24] indicates that the azomethine nitrogen is coordinated to the metal ion. The disappearance of the broad band due to H-bonded –OH stretching in the spectra of metal complexes gives evidence for the formation of M-O bonds via deprotonation. Further, the high-intensity band due to phenolic C-O at 1306–1305 cm^{-1} in the Schiff bases appeared as a medium- to high-intensity band in the 1331–1358 cm^{-1} region in the complexes. Rupini *et al.* and El-Sharief *et al.* have reported similar features of ν(C=N) and phenolic OH groups of the Schiff bases of formyl coumarin[24,25]. The presence of coordinated water molecules in the complexes are confirmed by a broad band around 3433–3449 cm^{-1} and two weak bands in the regions 800–750 and 720–700 cm^{-1} due to ν(OH) rocking and wagging modes of vibrations, respectively[24,26]. The new bands in the regions 381–375 and 524–480 cm^{-1} in all complexes are assigned to stretching frequencies of (M-O) and (M-N) bonds, respectively[27,28]. The unaltered position due to ν(C=O) in all the complexes confirms its non-involvement in coordination.

Thus, the IR spectral data provide strong evidence for complexation of the potentially tetradentate Schiff bases with the ONNO sequence.

NMR spectral study of Schiff bases

The Schiff bases have been characterized by ^{1}H and ^{13}C NMR spectra and also 2D ^{1}H-^{1}H HOMOCOSY (correlation spectroscopy) to ensure ligand purity in solution and elucidate the differently positioned proton and carbon. The ^{1}H NMR and ^{13}C NMR spectral data are produced in Table 3.

In the ^{1}H NMR spectrum of $\mathbf{H_2L^I}$, signals at 14.7 and 2.4 ppm are ascribed to phenolic –OH and aromatic –CH_3, respectively. A characteristic singlet proton signal at 9.42 ppm is assigned to –CH=N. In addition to these, the multiplet signals around 6.1–7.6 ppm are due to aromatic protons. In the case of $\mathbf{H_2L^{II}}$, the singlets at 14.3, 9.1, and 2.5 ppm are attributed to phenolic –OH, –CH=N, and aromatic –CH_3, respectively. In addition to these, the multiplet signals around 6.1–7.7 ppm and triplet around 2.1 ppm are due to aromatic and CH_2-CH_2 protons, respectively. In both Schiff bases, phenolic –OH proton signals disappeared after the addition of D_2O[29].

In the ^{13}C NMR spectra of $\mathbf{H_2L^I}$ and $\mathbf{H_2L^{II}}$, the signals appearing in the region 111.3–158.6 ppm are assigned to aromatic carbons. The signals at 172.8–165.6, 144.3–142.3, and 38.4–36.8 ppm are due to C=O, C=N, and CH_3, respectively. In the case of $\mathbf{H_2L^{II}}$ an additional signal at 21.4 ppm is ascribed to the carbon of CH_2-CH_2.

In the two-dimensional ^{1}H-^{1}H HOMOCOSY NMR spectra, the signals observed are due to the interaction of

Table 1. Elemental analysis of Schiff bases and their Co(II), Ni(II), and Cu(II) complexes along with molar conductance and magnetic moment data.

			M%		C%		H%		N%		Molar conductance (ohm^{-1} cm^2 mol^{-1})	
Comp. no.	Empirical formula	Color/yield (%)	Obsd	Calcd	Obsd	Calcd	Obsd	Calcd	Obsd	Calcd		μ_{eff} (BM)
$\mathbf{H_2L^I}$	$C_{28}H_{20}N_2O_6$	84	—	—	69.99	70.0	4.16	4.16	5.84	5.83	—	—
$\mathbf{H_2L^{II}}$	$C_{24}H_{20}N_2O_6$	82	—	—	66.74	66.66	4.63	4.63	6.47	6.48	—	—
1	$Co(C_{28}H_{18}N_2O_6).2H_2O$	Brown/68	10.29	10.29	58.63	58.63	3.14	3.14	4.88	4.88	19	4.9
2	$Co(C_{24}H_{18}N_2O_6).2H_2O$	Brown/67	11.18	11.19	54.65	54.64	3.42	3.41	5.32	5.31	18	4.75
3	$Ni(C_{28}H_{18}N_2O_6).2H_2O$	Yellowish green/71	10.13	10.14	58.73	58.74	3.15	3.14	4.88	4.89	22.5	3.3
4	$Ni(C_{24}H_{18}N_2O_6).2H_2O$	Yellowish green/73	11.01	11.02	54.74	54.75	3.42	3.42	5.33	5.32	23	3.1
5	$Cu(C_{28}H_{18}N_2O_6).2H_2O$	Dark green/69	10.91	10.92	58.23	58.23	3.12	3.11	4.86	4.85	29.7	1.74
6	$Cu(C_{24}H_{18}N_2O_6).2H_2O$	Dark green/68	11.85	11.86	54.24	54.23	3.41	3.38	5.27	5.27	27	1.75

Table 2. The important infrared frequencies (in cm^{-1}) of Schiff bases and their metal complexes.

Compound	Co-ordinated waterν(OH)	Lactonylν(C=O)	ν(C=N)	H-bonded–OHstretching	ν(C=C)	Phenolicν(C-O)	ν(M-N)	ν(M-O)
$C_{28}H_{20}N_2O_6$	—	1735	1613	3072	1585	1306	—	—
$C_{24}H_{20}N_2O_6$	—	1720	1632	3062	1585	1305	—	—
$Co(C_{28}H_{18}N_2O_6).2H_2O$	3439	1737	1602	—	1578	1355	524	381
$Co(C_{24}H_{18}N_2O_6).2H_2O$	3433	1721	1618	—	1579	1335	506	376
$Ni(C_{28}H_{18}N_2O_6).2H_2O$	3449	1736	1603	—	1580	1358	499	380
$Ni(C_{24}H_{18}N_2O_6).2H_2O$	3435	1721	1622	—	1580	1340	510	375
$Cu(C_{28}H_{18}N_2O_6).2H_2O$	3446	1735	1598	—	1582	1356	480	378
$Cu(C_{24}H_{18}N_2O_6).2H_2O$	3438	1720	1617	—	1581	1331	496	380

Table 3. The important ^{1}H NMR and ^{13}C NMR data for Schiff bases.

Schiff base no.	^{1}H NMR ($CDCl_3$) (ppm)	^{13}C NMR ($CDCl_3$) (ppm)
$\mathbf{H_2L^I}$	14.7 (s, 2H, OH), 9.42 (s, 2H, HC=N), 6.1–7.6 (m, 10H, Ar-H), 2.4 (s, 6H, Ar-CH_3)	111.3, 113.1, 118.6, 123.6, 125.5, 126.7, 131.5, 133.6, 138.2, 148.6, 152.2, 158.6, (aromatic carbon), 144.3 (C=N), 172.8 (C=O), 38.4 (CH_3)
$\mathbf{H_2L^{II}}$	14.3 (s, 2H, OH), 9.1 (s, 2H, HC=N), 6.1–7.7 (m, 6H, Ar-H), 2.5 (s, 6H, Ar-CH_3), 2.1 (t, 4H, CH_2-CH_2)	113.1, 118.6, 123.6, 125.5, 126.7, 131.5, 133.6, 138.2, 148.6, (aromatic carbon), 142.3 (C=N), 165.6 (C=O), 36.8 (CH_3), 21.4 (CH_2)

proton and proton, in which the proton values are recorded along both the *y*-axis and the *x*-axis. A representative two-dimensional NMR spectrum of $\mathbf{H_2L^I}$ is discussed here. The spectrum clearly included all the protons of the aromatic region observed as a cross peak in the region 6.1–7.7 ppm. The peaks due to CH=N and CH_3 were well resolved and a signal was observed at corresponding coinciding points of the *y*- and the *x*-axis.

Thus, the NMR results support the IR inferences of the Schiff bases.

Electronic spectra

The electronic spectra of the Co(II) complexes exhibited absorption bands in the region 8000–10,000 cm^{-1} and 18,000–20,000 cm^{-1}, corresponding to the transitions $^{4}T_{1g}$ (F) → $^{4}T_{2g}$ (F) (ν_1); $^{4}T_{1g}$ (F) → $^{4}T_{1g}$ (P) (ν_3), respectively. In the present investigation, brownish Co(II) complexes showed absorption bands around 9654–9648 and 18,865–18,876 cm^{-1}, corresponding to ν_1 and ν_3 transitions, respectively. These bands are characteristic of high-spin octahedral Co(II) complexes[26]. However, the ν_2 band was not observed because of its proximity to the strong ν_3 transition.

The greenish $Ni(C_{28}H_{18}N_2O_6).2H_2O$ complex exhibited three bands at 10,582, 16,393 and 26,178 cm^{-1}, attributed to the $^{3}A_{2g}$ → $^{3}T_{2g}$ (ν_1); $^{3}A_{2g}$ → $^{3}T_{1g}$ (F) (ν_2); and $^{3}A_{2g}$ → $^{3}T_{1g}$ (P) (ν_3) transitions, respectively, which indicate octahedral geometry around the Ni(II) ion. The ligand field parameters are presented in "Supplementary material" Table S1. The value of the ν_2/ν_1 ratio was found to be around 1.549, and the μ_{eff} value is around 3.167, which is within the range of 2.8–3.5 BM, suggesting the octahedral environment. The values of the nephelauxetic parameter, β, indicate the low covalent character of the metal–ligand σ bonds[30]. Hence, the ligand field parameters correlate with the electronic spectral and magnetic properties.

The electronic spectra of the Cu(II) complex displayed two prominent bands. A low-intensity broad band at 16,658 cm^{-1} is assignable to the $^{2}E_g$ → $^{2}T_{2g}$ transition. Another high-intensity band at 25,523 cm^{-1} is due to symmetry-forbidden ligand → metal charge transfer. On the basis of the electronic spectra, a distorted octahedral geometry around the Cu(II) ion is suggested[31].

Magnetic studies

The magnetic moments obtained at room temperature are listed in Table 1. The magnetic measurement for the Co(II) complexes showed magnetic moment values of 4.9 and 4.75, which are well within the range of 4.3–5.2 BM, and the Ni(II) complexes showed magnetic moment values of 3.3 and 3.1, within the range of 2.8–3.5 BM, suggesting[32,33] consistency with their octahedral environment. The Cu(II) complexes exhibited magnetic moment values of 1.74 and 1.75 BM, slightly higher than the spin-only value of 1.73 BM expected for one unpaired electron, which offers the possibility of a distorted octahedral geometry[34].

ESR spectroscopy

The ESR spectrum of a representative Cu(II) complex, $Cu(C_{28}H_{18}N_2O_6).2H_2O$, showed a g value of 2.00277. The $g_{\parallel}$ and $g_{\perp}$ values were found to be 2.0273 and 2.1240, respectively. The g_{av} was calculated to be 2.0919. The Cu(II) complex spectrum was reversed axial, with $g_{\perp} > g_{\parallel}$. The complex would thus have an essentially d_z^2 ground state, which suggests either a compressed tetragonal, *cis*-octahedral, or distorted octahedral structure[35,36]. Thus, the ESR spectral results provide further evidence to support the magnetic and electronic spectral results.

FAB-mass spectral studies of Schiff bases and their complexes

The FAB-mass spectrum of $\mathbf{H_2L^I}$ is depicted in "Supplementary material" Figure S1. The spectrum showed a molecular ion peak at *m/z* 480, which is equivalent to its molecular weight. In addition, the fragment peaks at *m/z* 465 and 292 are due to the cleavage of CH_3 and $C_{10}H_8O_3$, respectively. In the case of $\mathbf{H_2L^{II}}$ the molecular ion peak at *m/z* 432 is ascribed to $C_{24}H_{20}N_2O_6$. The peaks at 417 and 241 are assigned to the cleavage of CH_3 and $C_{10}H_8O_3$, respectively.

The FAB-mass spectra of Co(II), Ni(II), and Cu(II) complexes with $\mathbf{H_2L^I}$ showed a molecular ion peak M^+ at *m/z* 573, 572, and 577, respectively, equivalent to their molecular weights. All the fragments of the species $[ML.2H_2O]^+$ undergo demetallation to form the species $[L + 2H]^+$ giving a fragment ion at *m/z* 480. The fragmentation peaks observed in the case of $Cu(C_{28}H_{18}N_2O_6).2H_2O$ at 541, 354, 250, and 63 correspond to $2H_2O$, $C_{11}H_7O_3$, $C_6H_4N_2$, and $C_{11}H_7O_3$, respectively. Also, the species $[ML.2H_2O]^+$ undergoes demetallation to form the species $[L + 2H]^+$ giving a fragment ion at *m/z* 480. Similar features are evident for other complexes. All these fragmentation patterns were well observed in the FAB-mass spectra.

Thermal studies

The thermal behavior of Co(II), Ni(II), and Cu(II) complexes has been studied as a function of temperature. The thermal

behavior of all the complexes is almost the same. Hence, the representative $Co(C_{28}H_{18}N_2O_6).2H_2O$, $Ni(C_{28}H_{18}N_2O_6).2H_2O$, and $Cu(C_{28}H_{18}N_2O_6).2H_2O$ complexes are discussed.

The $Cu(C_{28}H_{18}N_2O_6).2H_2O$ complex is represented in "Supplementary material" Figure S2. The thermal decomposition of the Cu(II) complex took place in three steps as indicated by differential thermal gravimetry (DTG) curves around 205–255, 335–370, and 505–535°C, corresponding to the mass loss of coordinated water molecules, aminophenol, and formyl coumarin moieties, respectively. In the case of Co(II) and Ni(II) complexes, decomposition took place in three steps corresponding to the loss of coordinated water molecules, aminophenol, and formyl coumarin moieties around 210–240, 270–300, and 495–530°C, respectively. Both water molecules of all the complexes depart in a considerably narrow (~50 K) one-step process. This may be due to an easier diffusion of water molecules through the crystal lattice of the complexes. Finally, the metal complexes decomposed gradually with the formation of metal oxides above 535°C. The nature of the proposed chemical change with the temperature range and the percentage of metal oxide obtained are given in "Supplementary material" Table S2.

Electrochemistry

The cyclic voltammogram of the $Cu(C_{28}H_{18}N_2O_6).2H_2O$ complex is depicted in "Supplementary material" Figure S3. A cyclic voltammogram of the Cu(II) complex displayed two reduction peaks, the first at $E_{pc} = -1.5894$ V, with corresponding oxidation peak at $E_{pa} = 0.4938$ V, and a second at $E_{pc} = -2.3235$ V,with a corresponding oxidation peak at $E_{pa} = -0.2410$ V. The peak separation of the first couple ($\triangle E_p$) is 1.0956 V at 200 mV/s and that of the second couple is 2.0825 V. The most significant feature of the Cu(II) complex is the Cu(II)/Cu(I) couple, and the redox process proceeds through the formation of the radical ion. The difference between forward and backward peak potentials can provide a rough evaluation of the degree of reversibility of the one-electron transfer reaction. The analysis of cyclic voltammetric responses with varying scan rates 50–200 mV/s gave evidence for the quasi-reversible one-electron oxidation state ("Supplementary material" Figure S4). The ratio of cathodic to anodic peak height was less than one. However, the peak current increased with an increase of the square root of the scan rate. This establishes the electrode process as diffusion controlled[37]. The separation in peak potentials increased at higher scan rates. These characteristic features are consistent with the quasi-reversibility of the Cu(II)/Cu(I) couple.

Fluorescence spectroscopy

The emission spectra of the Schiff bases and the complexes were studied in DMF and DMSO.

$\mathbf{H_2L^I}$ is characterized by an emission band around 486 nm in DMF and 490 nm in DMSO ("Supplementary material" Figure S5), due to the formation of the phenoxide anion. Upon the addition of 2–3 drops of aqueous alkali (2% NaOH) to the Schiff base solution, we observed λ_{max} values at 458 nm in DMF and 461 nm in DMSO. In the case of $\mathbf{H_2L^{II}}$, an emission band around 472 nm in DMF and 477 nm in DMSO was observed. On the addition of 2–3 drops of aqueous alkali (2% NaOH) to the Schiff base solutions, we observed λ_{max} values at 446 nm in DMF and 452 nm in DMSO, respectively. The shift in λ_{max} values after the addition of 2–3 drops of aqueous alkali (2% NaOH) in both Schiff bases clearly indicates that the proton transferred (H-bonded ion pair) species exist in equilibrium[38,39].

The emission spectra of the Co(II), Ni(II), and Cu(II) complexes with $\mathbf{H_2L^I}$ were characterized by an emission band around 476/483 nm, 476/464 nm, and 501/501 nm in DMF/DMSO ("Supplementary material" Figure S6). In the case of Co(II), Ni(II), and Cu(II) complexes of $\mathbf{H_2L^{II}}$ emission bands were observed at 454 nm, 459 nm, and 462 nm, respectively, in DMF and at 455 nm, 461 nm, and 468 nm, respectively, in DMSO. The shift of the λ_{max} value of the complexes compared with the Schiff bases is possibly due to the deprotonation of the hydroxyl group.

Biological results

In vitro antibacterial and antifungal activity

The microbial results are systematized in Table 4. The antibacterial and antifungal studies suggested that all the Schiff bases were biologically active, and some of their metal complexes showed significantly enhanced antibacterial and antifungal activity. It is, however, known[40,41] that chelation tends to make Schiff bases act as more powerful and potent bactereostatic agents, thus inhibiting the growth of bacteria and fungi more than the parent Schiff bases. It is suspected that factors such as solubility, conductivity, dipole moment, and cell permeability mechanism (influenced by the presence of metal ions) may be possible reasons for the increase in activity.

In the antibacterial studies it was observed that both Schiff bases were potentially active against *E. coli, S. typhi*, and *S. aureus*. All the Co(II), Ni(II), and Cu(II) metal complexes showed much enhanced activity against *S. typhi*, and Cu(II) complexes exhibited promising results against *E. coli*. A most interesting finding was that both the Schiff bases and their metal complexes showed higher activity compared to the standard drug against *S. aureus*. Both the Schiff bases and their Co(II), Ni(II), and Cu(II) complexes were found to possess higher antifungal activity than antibacterial activity. The antifungal activity of synthesized Schiff bases and some of their complexes was close to that of the standard drug fluconazole (Table 4). It has been reported in the past that metal complexes with Schiff bases of formyl coumarin derivatives possess high antimicrobial activity[17,18,23,42–44].

The minimum inhibitory concentration (MIC) of some selected compounds, which showed significant activity against selected bacterial and fungi species, was also determined, and results are presented in Table 5. The MIC of these compounds indicated that they were most active in inhibiting the growth of the tested organisms at a 10 μg/mL concentration.

Table 4. Biological results for Schiff bases and their metal complexes.

		% Inhibition against bacteria				% Inhibition against fungi		
Compound	Conc. (μg/mL)	*E. coli*	*S. aureus*	*P. aeruginosa*	*S. typhi*	*A. flavus*	*Cladosporium*	*A. niger*
$C_{28}H_{20}N_2O_6$	25	6.97	17.14	2.63	26.19	84.31	53.84	47.61
	50	23.25	23.52	44.73	45.23	92.15	76.92	76.19
	100	95.34	38.2	50.00	59.52	96.07	87.17	88.09
$C_{24}H_{20}N_2O_6$	25	8.26	16.35	6.35	28.96	82.64	52.86	54.36
	50	25.36	25.36	41.98	44.96	88.96	71.56	75.93
	100	92.55	44.26	52.63	61.59	94.56	82.94	83.67
$Co(C_{28}H_{18}N_2O_6).2H_2O$	25	—	—	—	—	76.47	5.12	57.14
	50	13.95	4.41	15.7	33.33	80.39	28.2	69.04
	100	62.79	8.82	26.31	59.52	84.31	46.15	73.8
$Co(C_{24}H_{18}N_2O_6).2H_2O$	25	—	—	14.69	26.76	78.96	6.94	61.73
	50	16.35	15.63	16.98	44.96	88.56	36.57	75.91
	100	71.56	26.35	24.86	66.93	92.57	49.382	81.09
$Ni(C_{28}H_{18}N_2O_6).2H_2O$	25	—	30.88	—	30.95	5.88	66.66	—
	50	18.6	36.76	—	73.8	23.52	76.92	28.57
	100	37.2	47.05	7.89	83.33	41.17	79.48	50.00
$Ni(C_{24}H_{18}N_2O_6).2H_2O$	25	—	15.63	—	42.59	9.68	64.91	25.39
	50	36.35	22.65	15.63	76.91	36.86	78.35	44.86
	100	59.63	29.63	19.86	87.33	49.76	81.94	65.92
$Cu(C_{28}H_{18}N_2O_6).2H_2O$	25	55.81	7.35	52.63	—	56.86	41.02	35.17
	50	65.11	13.23	60.52	14.28	64.7	53.84	57.14
	100	83.72	22.05	71.05	42.85	78.43	92.36	83.33
$Cu(C_{24}H_{18}N_2O_6).2H_2O$	25	88.37	20.88	26.31	57.14	86.27	33.33	61.9
	50	90.69	20.58	26.31	64.28	92.11	66.66	66.66
	100	93.02	36.76	76.84	69.04	94.11	74.35	80.95
Gentamicin	25	86.04	5.88	81.57	61.9			
	50	88.37	7.35	86.84	71.4	—	—	—
	100	88.37	14.7	89.47	80.95			
Fluconazole	25					84.31	92.3	88.09
	50	—	—	—	—	94.1	94.87	92.85
	100					96.08	97.43	97.61
Control	100	100	100	100	100	100	100	100

Table 5. Minimum inhibitory concentration (μg/mL) of selected compounds against selected bacteria.

Compound	*E. coli*	*P. aeruginosa*	*S. typhi*	*A. flavus*	*Cladosporium*	*A. niger*
$C_{28}H_{20}N_2O_6$	10	10	25	10	10	10
$C_{24}H_{20}N_2O_6$	10	10	25	10	10	10
$Co(C_{28}H_{18}N_2O_6).2H_2O$	10	10	10	10	10	25
$Co(C_{24}H_{18}N_2O_6).2H_2O$	10	10	25	10	10	10
$Ni(C_{28}H_{18}N_2O_6).2H_2O$	25	10	10	25	10	10
$Ni(C_{24}H_{18}N_2O_6).2H_2O$	10	25	10	25	10	25
$Cu(C_{28}H_{18}N_2O_6).2H_2O$	10	10	25	10	10	10
$Cu(C_{24}H_{18}N_2O_6).2H_2O$	10	10	25	10	25	10
Gentamicin	10	10	10	—	—	—
Fluconazole	—	—	—	10	10	10

Electrophoretic analysis

Representative $Co(C_{24}H_{18}N_2O_6).2H_2O$ and $Cu(C_{24}H_{18}N_2O_6).2H_2O$ complexes were studied for their DNA cleavage activity by the agarose gel electrophoresis method, and results are presented in Figure 1.

The gel after electrophoresis clearly revealed that both complexes acted on DNA, as there was a molecular weight difference between the control and the treated DNA samples. A difference was observed in the bands of the complexes (lanes 1–4) compared to the control DNA of *E.coli* and *A. niger*. This indicated that the control DNA alone did not show any apparent cleavage, unlike the complexes. However, the nature of the reactive intermediates involved in DNA cleavage by the complexes is not clear. The results indicate the important role of metal in these isolated DNA cleavage reactions. As the compounds were observed to cleave DNA, it can be concluded that the compounds inhibited growth of the pathogenic organism by cleaving the genome.

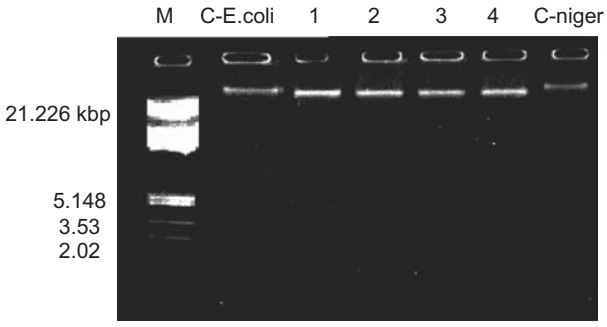

Figure 1. DNA cleavage study of Co(II) **(2)** and Cu(II) **(6)** complexes on genomic DNA. M, standard molecular weight marker; C- E.coli, control DNA of *E. coli*; lane 1, *E. coli* DNA treated with $Co(C_{24}H_{18}N_2O_6).2H_2O$; lane 2, *E. coli* DNA treated with $Cu(C_{24}H_{18}N_2O_6).2H_2O$; lane 3, *A. niger* DNA treated with $Co(C_{24}H_{18}N_2O_6).2H_2O$; lane 4, *A. niger* DNA treated with $Cu(C_{24}H_{18}N_2O_6).2H_2O$; C- niger: control DNA of *A. niger*.

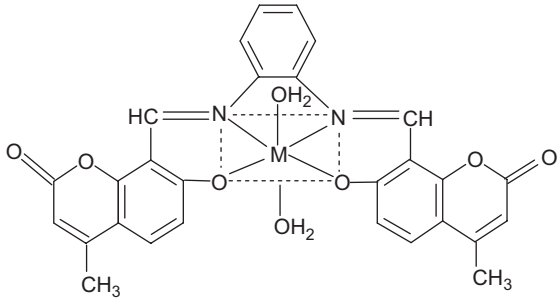

M	Formula	Complex no.
Co(II)	$Co(C_{28}H_{18}N_2O_6).2H_2O$	**1**
Ni(II)	$Ni(C_{28}H_{18}N_2O_6).2H_2O$	**3**
Cu(II)	$Cu(C_{28}H_{18}N_2O_6).2H_2O$	**5**

Figure 2. Structure of metal complexes **1**, **3**, and **5**.

Conclusions

The newly synthesized Schiff bases act as tetradentate ligands. The metal ion is coordinated through the azomethine nitrogen and phenolic oxygen atoms. The bonding of ligand to metal ion is confirmed by the analytical, spectral, magnetic, thermal, and fluorescence studies.

Biological study reveals that the Schiff bases and some metal complexes are highly active against *E. coli* and *S. typhi*. In antifungal studies, both Schiff bases and some of their complexes are found to be highly active. Co(II) **(2)** and Cu(II) **(6)** complexes show non-specific cleavage of DNA. The electrochemical properties of the metal complexes, investigated in DMF, show that the most significant feature of the Cu(II) complex is the Cu(II)/Cu(I) couple.

All these observations put together lead us to propose the following structures (Figures 2 and 3) in which the complexes have stoichiometry of the type $ML.2H_2O$ (M = Co(II), Ni(II), and Cu(II)).

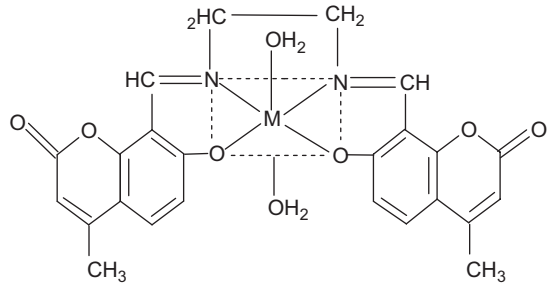

M	Formula	Complex no.
Co(II)	$Co(C_{24}H_{18}N_2O_6).2H_2O$	**2**
Ni(II)	$Ni(C_{24}H_{18}N_2O_6).2H_2O$	**4**
Cu(II)	$Cu(C_{24}H_{18}N_2O_6).2H_2O$	**6**

Figure 3. Structure of metal complexes **2**, **4**, and **6**.

Acknowledgments

***Declaration of interest*:** The authors report no conflicts of interest.

References

1. Egan D, O'Kennedy R, Moran E, Cox D, Prosser E, Thornes RD. *Drug Metab Rev* 1990;22:503–29.
2. Hoult Paya M. *Gen Pharmacol* 1996;27:713–22.
3. Laurin P, Ferroud D, Klich M, Dupuis-Hamelin C, Mauvais P, Lassaigne P, et al. *Bioorg Med Chem Lett* 1999;9:2079–84.
4. Connor DT. *US Patent*. 1981;126:287.
5. Emmanuel-Giota AA, Fylaktakidou KC, Hadjipavlou-Litina DJ, Litinas KE, Nicolaides DN. *J.Heterocyclic Chem* 2001;38:717–22.
6. Nofal ZM, El-Zahar M, Abd El-Karim S. *Molecules* 2000;5:99–113.
7. Manolov I, Danchev ND. *Eur J Med Chem Chim Ther* 1995;30:531–6.
8. Kirkiacharian S, Thuy DT, Sicsic S, Bakhchinian R, Kurkjian R, Tonnaire T. *Farmaco* 2002;57:703–8.
9. Yu D, Suzuki M, Xie L, Morris-Natschke SL, Lee KH. *Med Res Rev* 2003;23:322–45.
10. Marshall EM, Ryles M, Butler K, Weiss L. *J Cancer Res Clin Oncol* 1994;120:535–8.
11. Yanping Lia, Yanbo Wua, Jing Zhaoa, Yang Pin. *J Inorg Biochem* 2007;101:283–90.
12. Xiang-Li Wang, Hui Chao, Hong Li, Xian-Lan Hong, Liang-Nian Ji, Xiao-Yuan Li. *J Inorg Biochem* 2004;98:423–9.
13. Cowan JA. *Curr Opin Chem Biol* 2001;5:634–42.
14. Liu J, Zhang T, Lu T, Qu L, Zhou H, Zhang Q, et al. *J Inorg Biochem* 2002;91:269–76.
15. Vaidyanathen VG, Nair BU. *J Inorg Biochem* 2003;93:271–6.
16. Reddy PR, Rao KS, Satyanarayana B, Tetrahedron Lett. 2006;47:7311–7315.
17. Bagihalli GB, Avaji PG, Patil SA, Badami PS. J. Coord. chem. 2008;61:2793–2806.
18. Bagihalli GB, Avaji PG, Patil SA, Badami PS. *Eur J Med Chem* 2008;43:2639–49.
19. Ahluwalia VK, Bhagat P, Aggarwal R, Chandra R. *Intermediates for Organic Synthesis*. Delhi: I.K. International Pvt. Ltd., 2005.
20. Brown TA, Molecular biology- A practical approach, Oxford University Press, USA, Volume 1, 51–52, (1990).
21. Sadana AK, Mirza Y, Aneja KR, Prakash O. *Eur J Med Chem* 2003;38:533–6.
22. Patil SA, Kulkarni VH. Polyhedron. 1984;3(1):21–24.
23. Rehman SU, Chohan ZH, Gulnaz1 F, Supuran CT. *J Enzyme Inhib Med Chem* 2005;20:333–40.
24. Rupini B, Mamatha K, Mogili R, Ravinder M, Srihari S. J. *Indian Chem. Soc*. 2007;84:629–631.
25. El-Sharief AMS, Gharib EAA, Ammar YA. J. *Indian Chem. Soc*. 1983;LX:1017–1019.

26. Singh K, Barwa MS, Tyagi P. *Eur J Med Chem* 2006;41:147–53.
27. Dholakiya PP, Patel MN. Synth. React. Inorg., Metal-Org., and Nano-Met. Chem. 2002;32(4):819–829.
28. Nakamoto K. *Infrared Spectra of Inorganic and Coordination Compounds*. New York: Wiley-Interscience, 1970.
29. Emara Adel AA, Adly Omima MI. *Trans Met Chem* 2007;32:889–901.
30. Ayman K, El-Sawaf, Douglas X, West A, Fathy El-Saied, El-Bahnasawy MR *Trans Met Chem* 1998;23:649–55.
31. Huiyan Liu, Haiying Wang, Feng Gao, Dezhong Niu, Zaisheng Lu. *J Coord Chem* 2007;60:2671–8.
32. Rao TR, Prasad Archana. *Synth React Inorg Met Org Nano Met Chem* 2005;35:299–304.
33. Hankare PP, Naravane SR, Bhuse VM, Delekar SD, Jagtap AH. Indian J. Chem. 2004;43A:1464–1467.
34. Singh DP, Ramesh Kumar, Malik V, Tyagi P. *Trans Met Chem* 2007;32:1051–5.
35. McGregor KT, Halfield WE. *J Chem Soc Dalton Trans* 1974:2448–51.
36. Estes WE, Govel DP, Halfield WE, Hodgson DJ. Inorg. Chem., 1978;17:1415–1421.
37. Bard A-J, Izatt L-R, eds. *Electrochemical Methods: Fundamentals and Applications*, 2nd ed. New York: Wiley, 2001.
38. Mukherjee S. Indian J. Chem. 1987;26:1002–1005.
39. Avaji PG, Patil SA, Badami PS. *Trans Met Ch*em 2008;33:275–83.
40. Chohan ZH, Supuran CT, Scozzafava A. *J Enzyme Inhib Med Chem* 2004;19:79–84.
41. Chohan ZH, Praveen M. *Appl Organomet Chem* 2001;15:617–25.
42. Kulkarni A, Avaji PG, Bagihalli GB, Patil SA, Badami PS. *J Coord Chem* 2009;62:481–92.
43. Bagihalli GB, Patil SA, Badami PS. *J Enzyme Inhib Med Chem* 2009;24:381–94.
44. Bagihalli GB, Patil SA, Badami PS, J. Enzym. Med. Chem. 2009;24(03): 730–741.

Supplementary material

Table S1. Ligand field parameters of Ni(II) complexes with Schiff bases.

	Transitions (cm^{-1})			ν_2 calcd.			Distortion			μ_{eff} calcd.		
	ν_1	ν_2	ν_3	(cm^{-1})	Dq (cm^{-1})	B^1 (cm^{-1})	(%)	ν_2/ν_1	LSFE	(BM)	β	β° (%)
3	10,582	16,393	26,178	16,534	1058.2	731.126	0.858	1.549	36.281	3.167	0.692	30.765
4	10,565	16,376	26,145	16,511	1056.5	730.768	0.821	1.550	36.223	3.168	0.692	30.799

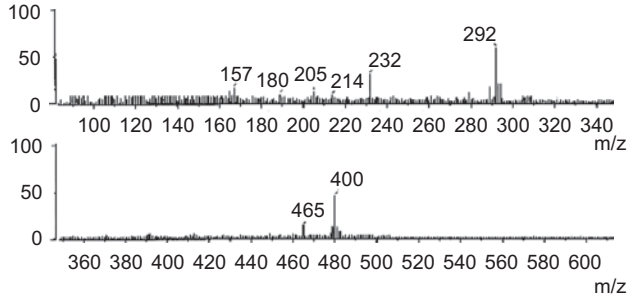

Figure S1. FAB mass spectrum of Schiff base I.

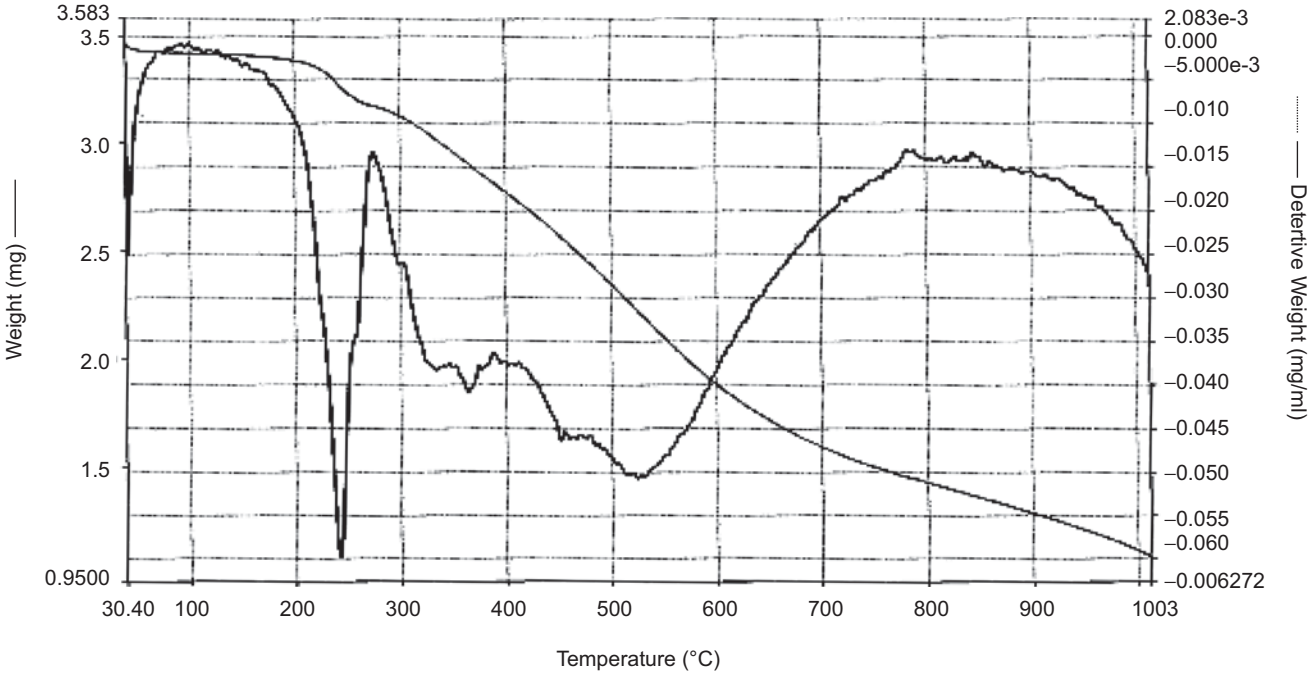

Figure S2. TG/DTG spectrum of Cu(II) **(5)** complex.

Table S2. Thermogravimetric data for Co(II) (**1**), Ni(II) (**3**), and Cu(II) (**5**) complexes.

	Metal oxide (%)		Decomposition	Weight loss (%)		
	Obsd	Calcd	temperature (°C)	Obsd	Calcd	Inference
$Co(C_{28}H_{18}N_2O_6).2H_2O$	10.289	10.296	210–240	6.263	6.28	Loss of coordinated water molecules
			275–300	18.148	18.15	Loss of diamine
			495–515	65.281	65.27	Loss of formyl coumarin
$Ni(C_{28}H_{18}N_2O_6).2H_2O$	10.141	10.139	210–235	6.286	6.29	Loss of coordinated water molecules
			270–295	18.176	18.18	Loss of diamine
			505–530	65.384	65.38	Loss of formyl coumarin
$Cu(C_{28}H_{18}N_2O_6).2H_2O$	10.913	10.918	205–255	6.232	6.239	Loss of coordinated water molecules
			335–370	18.02	18.024	Loss of diamine
			505–535	64.82	64.818	Loss of formyl coumarin

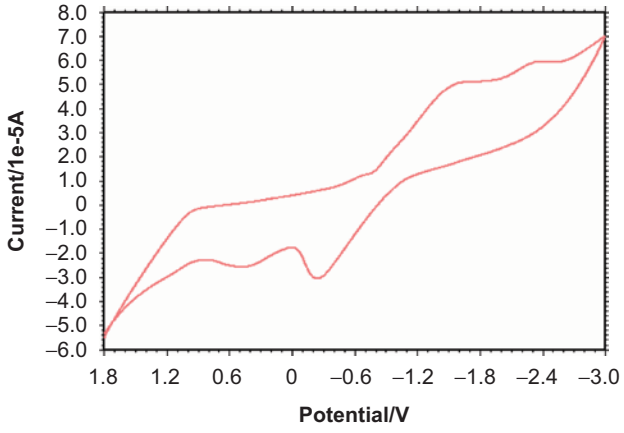

Figure S3. Cyclic voltammogram of $Cu(C_{28}H_{18}N_2O_6).2H_2O$ **(5)** with scan rate 200 mV/s.

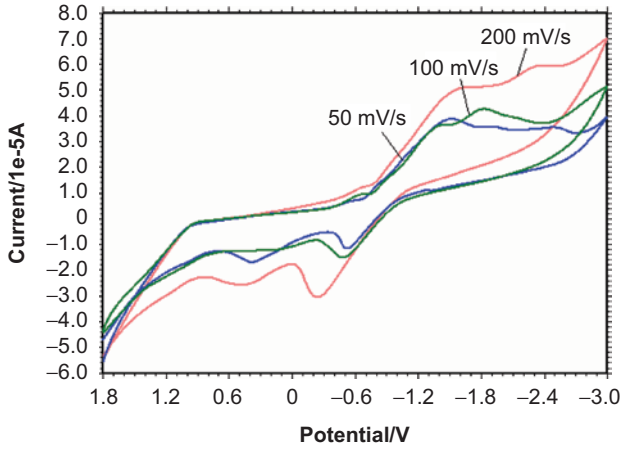

Figure S4. Cyclic voltammogram of Cu(II) **(5)** with scan rates 50, 100, and 200 mV/s.

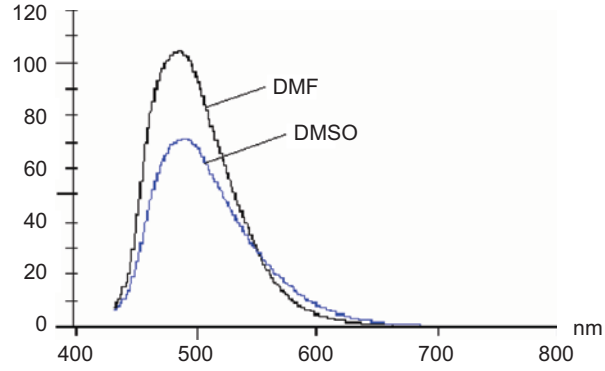

Figure S5. Emission spectrum of $\mathbf{H_2L^I}$ in DMF and DMSO.

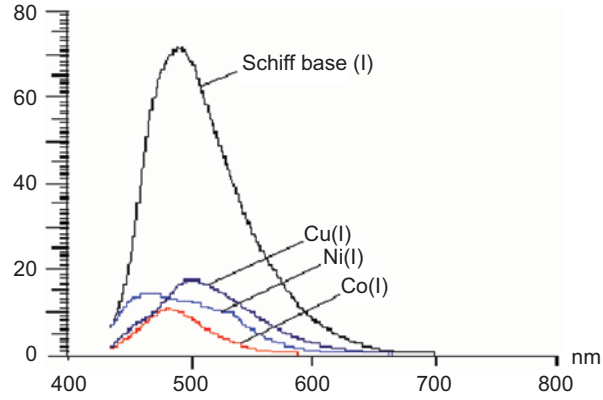

Figure S6. Emission spectrum of Co(II) **(1)**, Ni(II) **(3),** and Cu(II) **(5)** complexes with $\mathbf{H_2L^I}$ in DMSO.